

GROWTH OF ORGANIC FILMS ON SEMICONDUCTOR SURFACES:
FUNDAMENTAL REACTIVITY STUDIES AND
MOLECULAR LAYER DEPOSITION INVOLVING
ISOCYANATES AND ISOTHIOCYANATES

A DISSERTATION

SUBMITTED TO THE DEPARTMENT OF CHEMICAL ENGINEERING

AND THE COMMITTEE ON GRADUATE STUDIES

OF STANFORD UNIVERSITY

IN PARTIAL FULFILLMENT OF THE REQUIREMENTS

FOR THE DEGREE OF

DOCTOR OF PHILOSOPHY

Paul W. Loscutoff

July 2010

UMI Number: 3430511

All rights reserved

INFORMATION TO ALL USERS

The quality of this reproduction is dependent upon the quality of the copy submitted.

In the unlikely event that the author did not send a complete manuscript and there are missing pages, these will be noted. Also, if material had to be removed, a note will indicate the deletion.

UMI[®]

Dissertation Publishing

UMI 3430511

Copyright 2010 by ProQuest LLC.

All rights reserved. This edition of the work is protected against unauthorized copying under Title 17, United States Code.

ProQuest[®]

ProQuest LLC
789 East Eisenhower Parkway
P.O. Box 1346
Ann Arbor, MI 48106-1346

© Copyright by Paul W. Loscutoff, 2010

All Rights Reserved


PREVIEW

I certify that I have read this dissertation and that, in my opinion, it is fully adequate in scope and quality as a dissertation for the degree of Doctor of Philosophy.



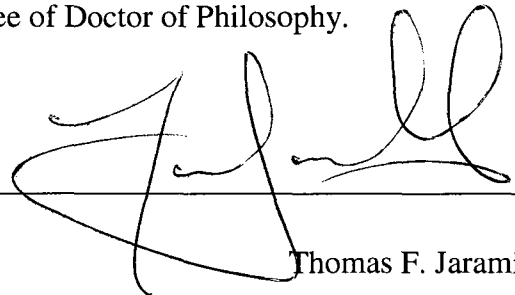
Stacey F. Bent, Principal Advisor

I certify that I have read this dissertation and that, in my opinion, it is fully adequate in scope and quality as a dissertation for the degree of Doctor of Philosophy.



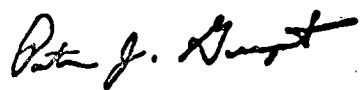
Zhenan Bao

I certify that I have read this dissertation and that, in my opinion, it is fully adequate in scope and quality as a dissertation for the degree of Doctor of Philosophy.



Thomas F. Jaramillo

Approved for the University Committee on Graduate Studies:



PREVIEW

ABSTRACT

The continued pursuit of smaller device dimensions by the semiconductor industry has led to an increased interest in functional organic films. Organics have great potential as advanced materials, owing to the versatility of organic moieties and vast knowledge base of organic reactivity. In order to implement organic films into semiconductor devices, the inorganic/organic hybrid interfaces must be investigated, so that the reactivity at these pivotal features is well-known. In this work organic films are studied in two environments: the Ge(100)-2×1 surface and the SiO₂ surface.

The reconstructed Ge(100)-2×1 surface offers a well-defined substrate, ideal for fundamental reactivity studies. Organic reactants are deposited under ultrahigh vacuum conditions, allowing reactions between gas-phase organic molecules and the surface to be isolated and analyzed by *in situ* spectroscopic techniques. By use of infrared (IR) spectroscopy, x-ray photoelectron spectroscopy (XPS) and density functional theory (DFT) modeling, we investigate the reactivity of phenyl and *tert*-butyl isocyanate and isothiocyanate at the Ge(100)-2×1 surface. The isocyanate and isothiocyanate moieties are both highly reactive groups consisting of a cumulated double bond containing two heteroatoms, allowing for many potential products with the Ge surface. We find that dative bonding through the heteroatoms plays an important role in the surface reactions, functioning as either reaction intermediates or final products depending on the adsorbate. Various cycloaddition products are also observed at the surface, with prominent reactivity trends resulting from the differences in oxygen and sulfur reactivity.

In order to study the practical implementation of organic films, molecular layer deposition (MLD) reactions are studied on the hydroxylated SiO₂ surface. MLD is a layer-by-layer technique, where films are deposited one molecular unit at a time, allowing for film tailorability and composition control down to single molecule specificity. Coupling reactions between isocyanate and isothiocyanate moieties with amines to form polyurea and polythiourea films, respectively, are studied. The MLD films are analyzed by *ex situ* ellipsometry, IR spectroscopy, XPS, and DFT. A constant growth rate and monomer dose saturation is observed for both the urea and thiourea coupling chemistry, and chemical composition of the films agrees well with theoretical

models. The ability to precisely control film composition is demonstrated through the deposition of polyurea blends, with a homogenous composition throughout the film, and polyurea laminates, with layers of distinct composition within the film. Organic films have shown promise as copper diffusion barrier layers, and the effectiveness of the MLD films as copper barrier layers is investigated through thermal stability, adhesion, and copper penetration measurements. The films demonstrate potential in this application, but further modification of the films is necessary to meet all the requirements necessary for barrier layer implementation. The thesis concludes with some perspectives on the future of organic films on semiconductors.

PREVIEW

ACKNOWLEDGMENTS

The completion of this thesis would not have been possible without the help and support of many people in my life. My family, friends, mentors, and teachers have all played key roles in shaping the scientist and engineer that I am today.

The details of a graduate career are determined largely by the research group and advisor, and I owe much thanks for my graduate experience to my advisor, Stacey Bent. The balance between hands-off and hands-on advising is a difficult one to find, but Stacey patiently allowed me to pursue research interests that led to growth as a scientist while still managing to steer me back on track when I strayed too far from the research goals. Although the design of a new reactor heater and building computers (including learning Linux) for reaction modeling may have been a bit of a stretch, I am more complete as a researcher by having been able to complete these projects. As my thesis indicates, in the course of my research I saw a sharp change in my field of interest, from fundamental reactions in ultrahigh vacuum (UHV) to the application-oriented molecular layer deposition (MLD) in rough vacuum. Building the (MLD) reactor, developing new MLD chemistries, and finding applications for MLD films in both photoresists and copper diffusion barriers are examples of situations that presented unique challenges, and I am thankful that Stacey helped guide me down a path that allowed me to address these issues in the course of my research.

The Bent Research Group changed significantly over the course of my graduate career, but the group members were always friendly and made my graduate experience enjoyable. Older group members, such as Mike Filler, Rong Chen, Neville Mehenti, Junsic Hong, and Xirong Jiang welcomed me into the group and answered many questions as I learned about how to be a successfully graduate researcher. I owe special thanks to Mike Filler, who showed me the ropes on the UHV chambers and invested many hours mentoring me during my initial time in the group, even as he was working hard to graduate. I can truly appreciate now the amount of time he put spent teaching me, never once making me feel like the burden I must surely have been as he was trying to finish up his own research. As Mike left Stanford, I was fortunate enough to have Jeff King join the group as a postdoc. Jeff picked up where Mike left off, and was

instrumental in teaching me (both directly and by example) about building reactors and approaching problems from a practical engineering perspective. I was also able to learn from Jeff's love of coffee, and would have never tried some of the more exotic types of coffee without his influence.

Jessica Kachian was my classmate and Bent Group cohort throughout my time at Stanford. Whether talking science, music, or the latest celebrity gossip, Jess made the office environment entertaining and an enjoyable place to work. As we both came into the group working on organic functionalization, we were able to share many successes and frustrations in our research, learning from each other and helping each other with chamber "surgery" when necessary. Pendar Ardalan and Jonathan Bakke were great officemates in the upstairs office, and I enjoyed our many conversations and rocking out to various genres of music. Jonathan was especially helpful in the automation of the MLD chamber, and I am grateful that I was able to learn from his experience in building a reactor and writing LabVIEW code to run the equipment. As the Bent Group has grown over time, there are now many people that I have interacted with on a daily basis, and I want to thank Marja Mullings, Nid Methaapanon, Tom Brennan, Han Zhou, Keith Wong, Sang-Wook Park, Art Wangperawong, Steve Herron, Jukka Tanskanen, Han-Bo-Ram Lee, Katie Pickrahn, and Bonggeun Shong. Keith and Jukka were especially helpful in the fundamental reactivity studies, with Keith continuing to seek the unifying theory of isocyanate reactivity and Jukka helping to understand the benefits and limitations of various quantum chemical methods.

Although it seems like a long time ago, my incoming class helped me get through the first two years of graduate school, including most of the coursework. It was invaluable to have a group of friends going through the same classes and offering each other help with problem sets and studying. Of the class, special thanks go to John Kirkwood, Becky Gerard, Chris McCormick and Jon Kuchenreuther, for their friendship. Jonny gets double credit, for being a great roommate for four years. Anders Berliner is an amazing person, and it is thanks to his organization of the intramural sports teams for the department that I was able to enjoy sports from basketball to wallyball to softball. I also owe him all credit for any improvement in my overall basketball skills, as I had to

learn tricks to beat him in our many one-on-one games. Socially, the class above me set a standard for friendly competition in everything from softball to Halo to Fantasy Football, and I want to thank Ajey Dambal, Chris Lueth, Jon Vroom, Bobby Feller, Mark Roberts, Curtiss Cobb, Collin Reese, and Jim Stapleton for fun times away from lab.

The Chemical Engineering Department is filled with outstanding professors and staff, and I would like to thank Professors Zhenan Bao and Thomas Jaramillo for being members of my reading committee. Without the department staff research would not be possible, and I would like to thank Jeannie Lewandowski, Jeanne Cosby, and Pam Juanes for all of their hard work to ensure that students have everything they need to complete their graduate work.

My friends and family are responsible for helping me get to Stanford in the first place, and I want to thank all of my friends from Berkeley and Davis for the support and friendship that they have given me throughout my life. I could not ask for a better family, and the years and years of support, encouragement, and laughter that I have shared with my sisters, cousins and more recently, in-laws and nephews, have been invaluable. My parents have always supported my efforts unconditionally, and I only hope that I can follow their example for encouraging my own children in the future.

Lastly and most importantly I want to thank my wife, Anna Sue, for helping me survive graduate school. She was encouraging and supportive throughout my entire graduate career, and always knew just the right things to say to keep me sane. Knowing that I would get to go home to her each night, no matter how my day in lab went, gave me a freedom that allowed me to get beyond any problem, no matter how stressful. She was unbelievably understanding about the time requirements of graduate research, and even came into lab with me on Saturdays, to keep me company while I ran experiments. She is my best friend, and this thesis is as much hers as it is mine.

TABLE OF CONTENTS

List of Tables.....	xiv
List of Figures.....	xv
Chapter 1. Introduction and Background.....	1
1.1. Group IV Semiconductor Surfaces.....	2
1.1.1. Oxides.....	2
1.1.2. Surface Reconstructions.....	5
1.2. Vacuum Deposition of Organic Films.....	8
1.2.1. Evaporation.....	8
1.2.2. Chemical Vapor Deposition.....	8
1.2.3. Self-Assembled Monolayers.....	10
1.3. Reactions at the Ge(100)-2×1 Surface.....	11
1.3.1. Nucleophilic/Electrophilic Reactions.....	12
1.3.2. Cycloaddition Reactions.....	15
1.3.3. Multiple Dimer Reactions.....	18
1.4. Molecular Layer Deposition.....	21
1.4.1 Introduction.....	21
1.4.2. Organic MLD Chemistries.....	23
1.4.3. Hybrid MLD Chemistries.....	25
1.5. Main Goals of Research.....	26
1.6. Organization of Thesis.....	29
1.7. Collaborations.....	30
1.8. References.....	30
Chapter 2. Analytical Methods.....	36
2.1. Surface Science and the Need for Vacuum.....	36
2.2. Ultrahigh Vacuum Chambers.....	37
2.3. Molecular Layer Deposition Reactor.....	38
2.4. Infrared Spectroscopy.....	40
2.4.1. Introduction.....	40

2.4.2. Theory.....	41
2.4.3. Transmission vs. Multiple Internal Reflection Geometries.....	42
2.4.4. Equipment.....	43
2.5. X-ray Photoelectron Spectroscopy.....	47
2.5.1. Introduction.....	47
2.5.2. Theory.....	47
2.5.3. Equipment.....	49
2.6. Ellipsometry.....	51
2.6.1. Introduction.....	51
2.6.2. Theory.....	51
2.6.3. Equipment.....	53
2.7. Quantum Chemical Calculations.....	54
2.7.1. Introduction.....	54
2.7.2. Basic Theory.....	55
2.7.3. Density Functional Theory.....	57
2.7.4. Basis Sets.....	58
2.7.5. Computational Details.....	60
2.8. References.....	62
Chapter 3. Reaction of Phenyl Isocyanate and Phenyl Isothiocyanate at the Ge(100)-2×1 Surface.....	64
3.1. Introduction.....	64
3.2. Experimental.....	67
3.3. Results and Discussion.....	69
3.3.1. Phenyl Isocyanate.....	69
3.3.2. Phenyl Isothiocyanate.....	74
3.3.3. Comparison of Reactivity.....	82
3.4. Conclusion.....	84
3.5. References.....	85

Chapter 4. Reaction of <i>Tert</i>-Butyl Isocyanate and <i>Tert</i>-Butyl Isothiocyanate at the Ge(100)-2×1 Surface.....	86
4.1. Introduction.....	86
4.2. Experimental.....	89
4.3. Results and Discussion.....	91
4.3.1. <i>Tert</i> -Butyl Isothiocyanate.....	91
4.3.2. <i>Tert</i> -Butyl Isocyanate.....	98
4.3.3. Comparison of Reactivity.....	107
4.4. Conclusion.....	109
4.5. References.....	110
Chapter 5. Molecular Layer Deposition of Polyurea Films.....	111
5.1. Introduction.....	111
5.2. Results and Discussion.....	114
5.3. Conclusion.....	130
5.4. Methods.....	131
5.4.1. Description of Materials and Reactor.....	131
5.4.2. Initial Surface Functionalization.....	132
5.4.3. Molecular Layer Deposition.....	132
5.4.4. Characterization Techniques.....	133
5.5. References and Footnotes.....	135
Chapter 6. Molecular Layer Deposition of Polythiourea Films.....	138
6.1. Introduction.....	138
6.2. Experimental.....	140
6.3. Results and Discussion.....	142
6.4. Conclusions.....	151
6.5. References.....	152
Chapter 7. Molecular Layer Deposition Films for Use as Copper Diffusion Barrier Layers.....	154
7.1. Introduction.....	154
7.2. Experiment.....	156

7.3. Discussion.....	157
7.3.1. MLD Film Design and Characterization.....	157
7.3.2. Copper Adhesion of MLD Films.....	160
7.3.3. Effectiveness of MLD Films as Copper Diffusion Barriers.....	162
7.4. Conclusion.....	164
7.5. References.....	165
Chapter 8. Conclusions and Perspectives.....	166
8.1. General Conclusions.....	166
8.2. The Future of Organic Films on Semiconductors.....	168
8.3. References.....	171
Appendix A. Time-Dependence of Phenyl Isocyanate at the Ge(100)-2×1 Surface.....	172
Appendix B. Reactivity of Ethyl Isocyanate at the Ge(100)-2×1 Surface.....	175
Appendix C. Molecular Layer Deposition of Polyurethane Films.....	180

LIST OF TABLES

Table 4.1. XPS binding energies, peak splitting and atomic composition for a saturation coverage of tBIC on Ge(100)-2×1.....	106
Table 5.1. Mode assignments for infrared spectra of 12 cycle PDIC/ED MLD film.....	120
Table 6.1. Vibrational modes associated with calculated frequencies, and corresponding peak frequencies in experimental spectra.....	146
Table 7.1. XPS relative atomic composition of MLD films, with theoretical values.....	159
Table 7.2. Adhesion values for various MLD films taken from 4-point bend testing.....	161

PREVIEW

LIST OF FIGURES

Figure 1.1. Standard RCA clean procedure, adapted from Plummer et. al. [11].....	4
Figure 1.2. Unit cell for the diamond cubic lattice crystal structure.....	5
Figure 1.3. Schematic of the (100) surface for Si and Ge showing the surface (a) unreconstructed, (b) reconstructed with symmetric dimers, and (c) reconstructed with tilted dimers.....	6
Figure 1.4. Extended surface ordering of the (100) reconstructions: The p(2×1) dimer reconstruction involving symmetric dimers; the c(4×2) dimer reconstruction with buckled dimers; and the p(2×2) dimer reconstruction with buckled dimers. The open circles represent the top-layer atoms, with the larger and smaller circles designating the up and down atoms of the dimer, respectively. The filled circles represent the next layer of atoms.....	7
Figure 1.5. Example VDP chemistries: (a) deposition of parylenes, (b) deposition of polypeptides, and (c) deposition of polyamides.....	9
Figure 1.6. Amine-terminated SAM formation, indicating the head group, backbone, and tail group of the SAM molecule.....	11
Figure 1.7. Dative bonding (a) between ammonia and boron trifluoride, and (b) between trimethylamine and the Ge(100)-2×1 dimer.....	13
Figure 1.8. Proton transfer reaction of ethanethiol at the Ge(100)-2×1 surface, with dative-bonded intermediate.....	14
Figure 1.9. Reaction of acetyl chloride with (a) methanol in solution, and (b) the Ge(100)-2×1 dimer in UHV.....	15
Figure 1.10. Various cycloaddition reactions on the Ge(100)-2×1 surface and their analogues in organic chemistry: (a) [2+2] cycloaddition, (b) [4+2] cycloaddition, (c) 1,3-dipolar cycloaddition, (d) group transfer.....	16
Figure 1.11. Bridging structure observed in the reaction of acetic acid with the Ge(100)-2×1 surface.....	19
Figure 1.12. Schematic of MLD system, showing sequential layering of bifunctional organic molecules.....	21
Figure 1.13. Schematic of the versatility of MLD films, showing (a) initial surface functionalization by a SAM, (b) regular repeating regions, (c) site-specific modification, (d) functional termination.....	23

Figure 1.14. Published MLD coupling chemistries. (a) reaction of dianhydrides with diamines to form polyimides [119; 124; 125; 148; 149], (b) reaction of dialdehydes with diamines to form polyazomethines [118; 146; 152], (c) reaction of dichlorides with diamines to form polyamides [120-123; 127], (d) reaction of diisocyanates with diamines to form polyureas [129], (e) reaction of diisocyanates with diols to form polyurethanes [134].....	24
Figure 1.15. Schematic of MLD sequence for SAM-based hybrid films, using 7-octenyltrichlorosilane (OTS) and titanium isopropoxide (TIP), starting from a hydroxylated surface.....	26
Figure 2.1. MLD chamber including manifold: (a) schematic and (b) picture.....	39
Figure 2.2. Schematic of MIR-IR geometry, including evanescent wave.....	43
Figure 2.3. Schematic of the Michelson interferometer.....	45
Figure 2.4. Stages of spectral processing: (a) interferogram, (b) single-beam spectrum, (c) absorbance spectrum, (d) H ₂ O and CO ₂ removal, and (e) baselining.....	46
Figure 2.5. Example of a hemispherical analyzer.....	50
Figure 2.6. (a) Schematic and (b) picture of the Gaertner L116C Ellipsometer.....	54
Figure 2.7. Plots of STO and GTO amplitude as a function of radial distance.....	59
Figure 2.8. Ge dimer clusters used in fundamental reactivity studies: (a) single-dimer cluster, (b) two-dimer row cluster, (c) two-dimer trench cluster.....	61
Figure 3.1. Potential surface products for the isocyanate and isothiocyanate groups reacting with the Ge(100)-2×1 surface dimer.....	66
Figure 3.2. FTIR spectra of PIC on Ge(100)-2×1 surface, showing a chemisorbed monolayer and physisorbed multilayer. DFT calculated vibrational spectra for the expected reaction products are given for comparison.....	70
Figure 3.3. Reaction coordinate diagrams for the CN [2+2], CO [2+2] and 1,3-dipolar cycloaddition products of PIC with the Ge(100)-2×1 surface.....	72
Figure 3.4. FTIR spectra of phenyl isothiocyanate on Ge(100)-2×1 surface, showing coverage dependence and multilayer.....	74
Figure 3.5. IR spectra calculated by DFT for PITC reaction products, with experimental spectra of 1 L and 10 L exposure given for comparison.....	76
Figure 3.6. Reaction coordinate diagrams for the CN [2+2], CS [2+2] and 1,3-dipolar cycloaddition products of PITC with the Ge(100)-2×1 surface.....	77
Figure 3.7. XPS fine scans for PITC for (a) N(1s), (b) S(2p), and (c) C(1s).....	80

Figure 3.8. Potential mechanism for reaction of the PITC 1,3-dipolar cycloaddition product to form a bridge-bonded sulfur atom with desorption of phenyl isonitrile.....	82
Figure 4.1. Potential surface products for <i>tert</i> -butyl isocyanate and isothiocyanate groups reacting with the Ge(100)-2x1 surface dimer.....	89
Figure 4.2. Chemisorbed and physisorbed FTIR spectra of tBITC on the Ge(100)-2x1 surface. Theoretical spectra for the expected products, calculated using DFT, are given for comparison.....	92
Figure 4.3. Reaction coordinate diagram for the expected products for the reaction of tBITC at the Ge(100)-2x1 surface, calculated by DFT.....	94
Figure 4.4. XPS fine scans of (a) C(1s), (b) N(1s), and (c) S(2p) electron energies for saturation coverage of tBITC on Ge(100)-2x1.....	97
Figure 4.5. FTIR spectra of tBIC physisorbed multilayer and chemisorbed layer with spectra after annealing the chemisorbed layer.....	99
Figure 4.6. Proposed schematic for C-N bond cleavage, resulting in surface-bound isocyanate and <i>tert</i> -butyl moieties.....	100
Figure 4.7. Reaction coordinate diagrams calculated by DFT for the expected reactions for tBIC with the Ge(100)-2x1 surface.....	102
Figure 4.8. Calculated IR spectra for stable tBIC products at the Ge(100)-2x1 surface. The experimental saturation spectrum is given for comparison.....	104
Figure 4.9. XPS fine scans for a saturation coverage of tBIC on Ge(100)-2x1 for the (a) C(1s), (b) N(1s), and (c) O(1s) electron orbitals.....	105
Figure 4.10. Major products for (a) tBITC and (b) tBIC at the Ge(100)-2x1 surface.....	107
Figure 5.1. MLD reaction using PDIC and ED, from an initial surface-bound amine....	114
Figure 5.2. Optimized geometry of the product of a hydrolyzed APTES chain reacting with PDIC and subsequently ED.....	115
Figure 5.3. (a) Plot of MLD film thickness as a function of number of cycles. Saturation curves showing growth rate as a function of (b) ED dose time (PDIC dose time fixed at 240 seconds) (c) PDIC dose time (ED dose time fixed at 10 seconds).....	117
Figure 5.4. TEM image of 15 MLD cycle sample with evaporated Cu coating on top of the organic film [55].....	119
Figure 5.5. FTIR spectra of MLD films of different total PDIC/ED cycles, and an IR spectrum calculated using DFT. Inset shows schematic of hydrogen bonding between adjacent organic chains.....	120

Figure 5.6. X-ray photoelectron spectra of survey scans for APTES film and 12 cycle PDIC/ED MLD film.....	122
Figure 5.7. X-ray photoelectron spectra for fine scans of 12 MLD cycle films: (a) N(1s) (b) O(1s) (c) C(1s).....	124
Figure 5.8. MLD growth rate for PDIC/ED system as a function of temperature.....	125
Figure 5.9. XPS spectra for MLD films with 30 cycles of PDIC/ED and PDIC/(ED+TBEA).....	127
Figure 5.10. Depth profiles for (a) laminate 1 with ED/TBEA/ED layering and (b) laminate 2 with TBEA/ED/TBEA layering. Theoretical film concentration is indicated by the dashed line. Error bars are based on XPS instrument uncertainty.....	120
Figure 6.1. Schematic of a polythiourea MLD cycle. An amine-terminated surface is exposed to PDITC to yield an isothiocyanate-terminated surface, which is exposed to ED to regenerate the amine-termination.....	142
Figure 6.2. (a) MLD film thickness as a function of increasing number of cycles, with saturation curves showing the growth rate dependence on (b) ED dose time and (c) PDITC dose time.....	143
Figure 6.3. Transmission FTIR spectra for increasing MLD cycles, with a calculated spectrum given for comparison.....	145
Figure 6.4. XPS fine scans of 12 cycle MLD films for the (a) N(1s), (b) S(2s), and (c) C(1s) core levels.....	147
Figure 6.5. TEM image of polythiourea MLD film on silica nanoparticle.....	149
Figure 6.6. FTIR spectra of MLD film after 20 min. vacuum anneals.....	150
Figure 7.1. (a) Polyurea monomers. (b) Schematic of polyurea film as copper diffusion barrier.....	158
Figure 7.2. FTIR spectra of annealed films for (a) PDIC/ED and (b) PDITC/ED.....	160
Figure 7.3. ToF SIMS spectra of 4-point bend test failure interfaces for 10 nm PDIC/ED sample with copper overlayer for the (a) epoxy side and (b) sample side.....	162
Figure 7.4. TEM images of PVD copper on (a) 10 nm PDIC/ED on 1 nm SiO ₂ , (b) 10 nm PDIC/TBEA on 4 nm SiO ₂ , and (c) 12 nm PDITC/ED on 4 nm SiO ₂	163

Figure A.1. FTIR spectra of PIC at the Ge(100)-2×1 surface for both non-isotopic PIC with ¹⁴ N and isotopic PIC with ¹⁵ N. Multilayer, saturation, DFT and time dependence spectra are given. Both absolute (relative to the clean surface spectrum) and difference (relative to initial saturation spectrum) spectra are given for time dependence.....	173
Figure B.1. FTIR spectra of EIC at the Ge(100)-2×1 surface showing time dependence after a saturation dose, a second saturation dose, and a DFT calculated spectrum of EIC for reference.....	176
Figure B.2. Three possible products for the reaction of EIC with the Ge(100)-2×1 surface: the CN [2+2] cycloaddition reaction product, the αCH dissociation product, and the αCH dissociation with βCH dissociation to form an OH group.....	176
Figure B.3. Theoretical IR spectra calculated by DFT for possible products of EIC at the Ge(100)-2×1 surface, with experimental saturation spectrum for comparison.....	178
Figure B.4. Reaction pathways calculated by DFT for expected products of EIC at the Ge(100)-2×1 surface.....	179
Figure C.1. Film thickness vs. cycle number for PDIC/EG MLD films.....	181
Figure C.2. FTIR spectra for PDIC/EG films with DFT calculated spectrum.....	182

PREVIEW

CHAPTER 1. INTRODUCTION AND BACKGROUND

From the discovery of the integrated circuit by Kilby and Noyce in 1959 [1], to present day microelectronics, the technology of the semiconductor industry has progressed at a remarkable rate. In 1962, those first integrated circuits consisted of 10 features [2]. Today, a single integrated circuit contains over one billion transistors, with linear features on the 10 nm scale [3]. This rapid size scaling of microelectronics follows Moore's Law [2], which predicts that the transistor density will double every two years. The ability to keep pace with Moore's Law for nearly 4 decades has only been possible by constant innovation in the areas of materials chemistry and process technology.

As the dimensions of semiconductor devices approach the atomic scale, materials properties and requirements change. An example of such a change occurred recently for the transistor gate dielectric. With the scaling of transistor dimensions, the SiO₂ dielectric was only 1.2 nm thick at the 65 nm technology node [4], a thickness that allowed for a leakage current of electrons to pass through the dielectric, inhibiting device performance. To correct for this problem, a hafnium-based dielectric was created, which with a higher dielectric constant, κ , was able to provide better electronic properties at thicker physical dimensions. Deposition of this new gate dielectric was only made possible by advances in science, specifically the thin film deposition method of atomic layer deposition (ALD) [3; 4]. While the gate dielectric problems have been solved for the time being, similar issues are being encountered throughout semiconductor device development, in areas from the channel material, to the photoresists, to the interconnects. Solving these problems will require materials and interface innovation, such that the progress of the microelectronics industry can continue to meet the standard set forth in Moore's Law.

This thesis looks at a relatively recent method for modifying semiconductor interfaces: the use of organic thin films. It is in the interfacial bonding that organic functionalization shows promise. The diverse library of organic functional groups allows for a tailoring of the interface properties by changes to the organic molecules used, and brings a new dimension to traditional, inorganic semiconductor devices. The potential applications for these organic layers are many, and cover a broad array of fields, including copper diffusion barriers [5; 6], chemical sensors [7], organic electronics [8; 9],

and adhesion promoters [10; 11]. With such a large degree of inherent tailorability, organic functionalization is poised to become a staple in future semiconductor devices.

This chapter provides an introduction and background for some important concepts in organic functionalization of semiconductors, and details the structure of the thesis. An initial overview of group IV semiconductor surfaces is given, followed by an overview of organic films on these surfaces. A more specific background is provided for the experimental systems discussed in the thesis: organic functionalization of the Ge(100)-2×1 surface, and low vacuum molecular layer deposition of organic films. Following these background sections, the main goal of the research and organization of the thesis are presented. The chapter concludes with a section detailing the collaborations that contributed to the thesis research.

1.1. Group IV Semiconductor Surfaces

Of the many semiconductor materials, silicon and germanium have found particular success in the microelectronics industry. These elements are both found in Group IV of the periodic table, and as congeners, they share the same valence electron configuration. They have the advantage of being elemental solids, and growth of large single crystals is done with ease by several refining methods [12]. Since integrated circuits are built up from semiconductor substrates, it is on the surfaces of Si and Ge that devices are formed. These surfaces become key interfaces within a device structure, and can often dominate the electronic behavior of the device. Here we look at two surfaces of these Group IV semiconductors: the oxide surface and the clean, reconstructed surface.

1.1.1. Oxides

Both germanium and silicon form insulating oxides when exposed to oxygen. Native silicon oxide (SiO_2) is a stable layer that offers substantial chemical resistance, acts as a good electrical insulator, and forms a low defect interface with Si [13]. In fact, the chemical, mechanical, and electrical properties of silicon oxide are nearly ideal for device formation [12]. These beneficial properties are the main reason that silicon has been the semiconductor of choice for history of the integrated circuit [1]. Thermal oxide growth occurs readily for silicon at temperatures as low as room temperature, where

exposure to ambient air will result in a native oxide with a thickness of 1-2 nm, depending on the initial surface treatment [12]. The thermal stability of SiO_2 is demonstrated in that oxidation followed by a high temperature anneal results in growth of SiO_2 from suboxides [14; 15]. An oxide can also be grown by direct oxidation of a heated Si substrate [12].

On the other hand, native germanium oxide (GeO_2), which is formed by leaving germanium in ambient atmosphere, has less desirable properties. GeO_2 is water soluble and forms a poor interface with Ge, which results in facile removal of the oxide layer and a high density of electronic defects [16]. Vacuum oxidation of Ge by O_2 results in growth of the Ge 1+, 2+ and 3+ oxidation states, but little or no growth of the 4+ state (GeO_2), and upon a high temperature anneal, all states, including GeO_2 , disappear at the expense of the 2+ state [17; 18]. GeO desorbs completely from the surface at 450 °C, and thus annealing above this temperature results in the oxide-free surface [18]. The low thermal stabilities and high defect densities make the germanium oxides unsuitable for use in transistor applications.

Cleaning of the silicon surface is a key step in semiconductor processing. The wafer cleaning process removes all contaminants from the semiconductor surface, and includes stripping away organics, metals, and even the oxide layer. The industry standard for device-level cleaning is the "RCA clean" and was originally developed at RCA labs by Kern and Puotinen in 1970 [19]. The standard implementation of the RCA clean is given in Figure 1.1, as adapted from Plummer et. al. [12]. The first step in the procedure is a $\text{H}_2\text{SO}_4/\text{H}_2\text{O}_2$ piranha solution, which is used to remove organic contaminants. The second step is to remove the oxide layer using a $\text{H}_2\text{O}/\text{HF}$ etch. After a deionized water (DI) rinse, the substrate is exposed to the SC-1 solution, a high pH mixture of $\text{H}_2\text{O}/\text{H}_2\text{O}_2/\text{NH}_4\text{OH}$, which removes heavy metals and oxidizes the substrate and any organic that was at the Si interface. Following a second DI rinse is the SC-2 solution, which is a low pH mixture of $\text{H}_2\text{O}/\text{H}_2\text{O}_2/\text{HCl}$, designed to remove alkali ions and cations that were not removed by the SC-1 step. Overall, the steps of the RCA clean have been proven to result in a contaminant free Si surface and oxide, allowing for device